Evidence for Early Evolution of Sulfated Peptide Signaling in Plant Development

Devin V. Tulio[1], Alexandra M. Shigenaga[2,3], Shu-Zon Wu[1], Pamela C. Ronald[2,3], Magdalena Bezanilla[1]*

1. Department of Biological Sciences, Dartmouth College, Hanover, NH 03755
2. Department of Plant Pathology, University of California, Davis, CA 95616
3. The Genome Center, University of California, Davis, CA 95616

* Corresponding Author

Abstract

In plants, the cell wall fixes the position of each cell; therefore, during development, plants rely on cellular proliferation and expansion for tissue patterning and organ formation. How plant cells communicate with neighboring cells to coordinate expansion for properly patterned tissues and organs is not well understood. In seed plants, organ growth is known to be modulated by sulfotyrosyl peptide signaling. Here, we report that the activity of TYROSYL PROTEIN SULFOTRANSFERASE (TPST), which is responsible for the post-translational modification of sulfotyrosyl peptides, is essential for expansion during development in the non-vascular plant, *Physcomitrium patens*. Plants that harbor a null mutation in the gene encoding TPST (*Δtpst*) were smaller, and while they formed gametophore initials, the gametophores did not fully expand. Mutational analysis of *P. patens* TPST identified the residue Histidine 124, a candidate catalytic residue, as essential for TPST function. Notably, addition of the sulfated signaling peptide, PSY1 from either *P. patens* or *Arabidopsis thaliana*, rescued all *Δtpst* developmental deficits. Taken together, these data suggest that TPST functions to sulfate PSY, and this activity is necessary for plant growth and development. Furthermore, since addition of AtPSY fully rescues *Δtpst* and PpPSY promotes root elongation in Arabidopsis and rice, these findings suggest that PSY signaling is evolutionarily conserved.

Introduction

In multicellular organisms, development involves cell proliferation, expansion, and differentiation. Unlike animal cells, plant cells are unable to undergo cell migration due to their encasement in a semi-rigid cell wall. Thus, the ultimate body shape depends on patterns of cell division and cell expansion (Cosgrove, 2005). How plant cells coordinate expansion with neighboring cells to shape tissue development and organ formation is not known.

Tyrosine-sulfated peptide signaling regulates plant growth, development, and immune response (Kaufmann and Sauter, 2019). A member of the PLANT PEPTIDE-

29 CONTAINING SULFATED TYROSINE (PSY) family, mature PSY1 is an 18-amino acid tyrosine-
30 sulfated peptide. Exogenous PSY1 at nanomolar concentrations enhances cellular
31 expansion and proliferation in Arabidopsis (Amano *et al.*, 2007) and overexpression or
32 exogenous application of PSY1 promotes root elongation in Arabidopsis and rice (Amano *et*
33 *al.*, 2007; Pruitt *et al.*, 2017; Ercoli *et al.*, 2024; Shi *et al.*, 2024). Other characterized
34 sulfopeptide hormones include PHYTOSULFOKINE (PSK), a 5-amino acid tyrosine-sulfated
35 peptide that functions with the plant hormones auxin and cytokinin to mediate cell cycle
36 reentry (Matsubayashi and Sakagami, 1996; Matsubayashi *et al.*, 1999), ROOT MERISTEM
37 GROWTH FACTORS (RGFs), and CASPARIAN STRIP INTEGRITY FACTORS (CIFs) (Matsuzaki
38 *et al.*, 2010; Doblas *et al.*, 2017; Nakayama *et al.*, 2017). However, the molecular
39 mechanisms that link tyrosine-sulfated peptides to cell expansion are not well understood.

40 Sulfated signaling peptides are processed and post-translationally modified from
41 precursor peptides. The prepropeptide amino-terminal signal peptide is cleaved during
42 secretion in the endoplasmic reticulum, and then it moves to the Golgi for tyrosine
43 sulfation and other modifications as appropriate. Propeptides are then transported, likely
44 to the apoplast, and become mature sulfated signaling peptides when they are cleaved at
45 the amino- and carboxyl-termini by largely unknown proteases (Kaufmann and Sauter,
46 2019).

47 Sulfotyrosine (sTyr) residues are formed by TYROSYL PROTEIN SULFOTRANSFERASE
48 (TPST) in the Golgi and are critical for certain protein-protein interactions in animals and
49 plants (Stewart and Ronald, 2022). TPST catalyzes sulfate transfer from adenosine 3'-
50 phosphate 5'-phosphosulfate (PAPS) to the hydroxyl group of specific tyrosyl residues
51 (Stewart and Ronald, 2022). Both TPST and soluble sulfotransferase sequences contain a
52 residue (Glu or His) whose side-chain provides the catalytic base, as well as PAPS-binding
53 residues in two conserved motifs, the 5' phospho-sulfate binding (5'-PSB) and the 3'
54 phosphate binding (3'-PB) elements (Stewart and Ronald, 2022). Although these conserved
55 elements were not initially identified in the plant TPST sequence (Komori *et al.*, 2009),
56 recent analysis detected putative PAPS-binding motifs (Stewart and Ronald, 2022). AtTPST
57 is a type I transmembrane protein, with a single membrane spanning segment and the

58 carboxyl-terminus exposed to the cytosol. In contrast, animal TPST is a type II
59 transmembrane protein, with the amino-terminus exposed to the cytosol. These different
60 topologies and apparent absence of sequence similarity suggested that plant and animal
61 TPSTs evolved independently via convergent evolution (Komori *et al.*, 2009).

62 In Arabidopsis, TPST is expressed throughout the plant but most highly at the root
63 apical meristem (Komori *et al.*, 2009). An Arabidopsis *tpst* null mutant displays various
64 developmental and growth phenotypes, including dwarfism and early senescence (Komori
65 *et al.*, 2009). TPST-mediated sulfation of tyrosine residues in PSYs, PSKs, RGFs, and CIFs is
66 critical for high-affinity binding to their cognate receptors (Kaufmann and Sauter, 2019;
67 Stewart and Ronald, 2022). The plant *TPST* gene is conserved from angiosperms to mosses
68 (Zhao *et al.*, 2019).

69 The spreading earth moss *Physcomitrium patens* is a tractable model for
70 understanding early events in plant evolution (Rensing *et al.*, 2020). Unlike angiosperms,
71 whose genomes encode four classes of sTyr peptides (PSK, PSY, RGF, and CIF), which have
72 multiple paralogs in each class, thus far the *P. patens* genome has been found to only
73 encode one copy of *PSY* and one copy of *PSK* (Furumizu *et al.*, 2021). Although two
74 immune-responsive PSY-like peptides in *P. patens* were recently identified (Lyapina *et al.*,
75 2025). In addition to the ease of genome editing, *P. patens* is predominantly haploid and
76 undergoes expansion in two main ways: in juvenile stages, protonemal filaments expand
77 via tip growth, and in adult tissues, gametophores form, in which the phyllids, or the leaf-
78 like structure, expand using diffuse growth (Schumaker and Dietrich, 1998). By analyzing
79 TPST function in *P. patens*, we can not only understand the role of sulfation in a system with
80 fewer predicted sulfo-peptides, but also investigate both diffuse and tip growth. Thus, *P.*
81 *patens* provides a platform from which to study plant TPST, such as identifying catalytic
82 residues and defining substrate specificity determinants. Here we report that tyrosine-
83 sulfated peptides are required for development, that the catalytic residue found in animal
84 sulfotransferases is conserved in *P. patens*, and that PSY signaling-induced expansion is
85 evolutionarily conserved.

Results

Sulfated peptides are required for development

To investigate the role of *TPST* (Pp3c16_24250) in cellular proliferation and development, we generated a null mutant using CRISPR/Cas9-mediated genome editing. *TPST* in *P. patens* has several predicted gene models, leading to two main predicted transcripts (Fig. S1A). The annotation in Phytozome suggests that both transcripts encode a single-pass type I transmembrane protein similar to Arabidopsis TPST (Komori *et al.*, 2009; Goodstein *et al.*, 2012; The UniProt Consortium, 2025). Additionally, both transcripts encode the same predicted signal peptide sequence. The only major difference between the two predicted proteins is the number of amino acids between the PAPs-binding catalytic region and the transmembrane domain (Fig. S1C). Both the short and long transcripts were detected using RT-PCR (Fig. S1B). Sequencing confirmed that the long transcript matches the predicted gene model V3.5, and the short transcript matches the predicted gene model V3.1. Therefore, we targeted a region of the locus corresponding to the amino-terminal coding region to create a *tpst* null mutant regardless of transcript length.

Two independent *tpst* null mutant lines were recovered, each resulting from a frameshift near the protospacer cut site (Fig. S1A). Both null mutants were smaller than wild-type plants (Fig. S1D and S1E). *Δtpst-6* was selected for future study and is subsequently referred to as *Δtpst*.

We found that *Δtpst* plants had very short protonemata, had a dark center, appeared denser than wild type, and were very round (Fig. 1A). 14-day-old *Δtpst* plants regenerated from protoplasts were 48% smaller than wild type ($p < 0.0001$) (Fig. 1B). In more mature plants, *Δtpst* was unable to form expanded gametophores and instead appeared to abort growth once a bud was formed (Fig. 1C). As the plant continued to develop, *Δtpst* turned brown before wild type, an indication of early senescence (Fig. 1D).

113 These data demonstrate that *TPST* function is critical for multiple aspects of *P. patens*
114 development, including protonemal growth, gametophore expansion, and senescence.

115

116 ***Catalytic residues are conserved in PpTPST***

117 Candidate 5'-PSB, 3'-PB, and catalytic base residues were identified in plant TPST
118 sequences (Stewart and Ronald, 2022) (Fig. 2A). We therefore used CRISPR/Cas9 and
119 homology-directed repair to generate Ala substitutions at three residues: Arg-81 in the
120 putative 5'-PSB element, Arg-144 in the putative 3'-PB element, and His-124, the putative
121 catalytic base (Fig. S2). Quantitative growth assays revealed that all three mutants (*tpst-*
122 *R81A*, *tpst-H124A* and *tpst-R144A*) were significantly smaller than the wild type ($p < 0.001$)
123 but were not significantly different from the *Δtpst* mutant or each other (Fig. 2C). This
124 indicates that all three mutants had compromised TPST activity. However, there were
125 differences in protonemal morphology amongst the mutants. The *tpst-H124A* mutant was
126 dense, round, and had short protonemata, similar to the *Δtpst* mutant (Fig. 2B). In contrast,
127 the *tpst-R81A* and tpst-*R144A* mutants were less dense and exhibited long protonemal
128 extensions.

129 To quantify these differences in plant morphology, we measured the circularity of
130 each plant. Circularity is proportional to the ratio of the area to the square of the perimeter.
131 The more the protonemata extend from the center of the plant, the lower the ratio. Wild-
132 type plants had an average circularity of 0.0182. *Δtpst* and *tpst-H124A* plants had
133 significantly higher circularity values of 0.0344 and 0.0333, respectively, whereas *tpst-*
134 *R81A* (0.0210) and *tpst-R144A* (0.229) displayed intermediate values (Fig. 2D). These
135 results demonstrate that the *tpst-H124A* alteration phenocopied the protonemal defect of
136 the *Δtpst* null allele, whereas the *tpst-R81A* and *tpst-R144A* alterations conferred an
137 intermediate phenotype.

138 To assess whether these alterations affect gametophore development or
139 senescence, we continued to monitor the growth and development of the mutants. After 8
140 weeks, the *Δtpst* and *tpst-H124A* mutants exhibited early senescence in comparison to the

141 wild type, the *tpst-R81A* and *tpst-R144A* mutants (Fig. 2E). Additionally, the *tpst-H124A*
142 mutant, like the *Δtpst* mutant, did not form expanded gametophores. In contrast, some
143 *tpst-R81A* and *tpst-R144A* mutant plants formed fully expanded gametophores throughout
144 the entirety of the plant, whereas other *tpst-R81A* and *tpst-R144A* mutant plants only
145 formed gametophores in part of the plant (Fig. 2E). Together, these results suggest that the
146 R81A and R144A alterations have lost some TPST function. In contrast, the H124A and
147 *Δtpst* alterations are indistinguishable, indicating that residue His-124 is essential for TPST
148 function.

149

150 ***PSY is evolutionarily conserved***

151 Because *Δtpst* plants cannot produce sulfated peptides, we investigated whether
152 exogenous application of *P. patens* PSY1 (PpPSY1), *A. thaliana* PSY1 (AtPSY1), and *A.*
153 *thaliana* PSK1(AtPSK1) synthetic peptides could alter the *Δtpst* phenotype. Initially, we
154 exposed 8-day-old tissue regenerated from protoplasts to peptides for 12 days and
155 screened for gametophore formation. The Δ*tpst* mutant formed fully expanded
156 gametophores after exposure to 200 nM of AtPSY1 or 1 μM of PpPSY1, but not to 200 nM of
157 AtPSK1 (Fig. 3). To observe fully expanded gametophores in *Δtpst*, we used a higher
158 concentration of PpPSY1 compared to AtPSY1.

159 To quantify the peptide-mediated rescue of protonemal growth in *Δtpst*, we moved
160 7-day-old plants regenerated from protoplasts to media supplemented with AtPSY1 or
161 PpPSY1. After five days of peptide treatment, *Δtpst* plants closely resembled wild type (Fig.
162 4A). Interestingly, wild-type plants grown on either peptide were significantly larger than
163 wild-type plants in the absence of peptide (Fig. 4B). There was no significant difference
164 between the *Δtpst* and wild-type plants grown on AtPSY1 ($p > 0.05$). When grown on
165 PpPSY1, *Δtpst* plants were the same size as the wild-type controls. However, in comparison
166 to all other peptide conditions, *Δtpst* grown on PpPSY1 were the smallest. These
167 observations support that the PpPSY1 peptide is less effective at rescuing *Δtpst* than
168 AtPSY1.

We continued to transfer the protoplast-regenerated plants on cellophane to fresh peptide media every week and confirmed our previous results that in the presence of either peptide, *Δtpst* exhibits normal gametophore development. As the protoplast-regenerated plants continued to age, we found that *Δtpst* turned brown around 7 weeks after protoplasting (tissue that is grown on cellophane behaves differently than tissue that is moved directly onto media). However, *Δtpst* grown on peptide media remained green, similar to wild type, suggesting that in the presence of the peptide, *Δtpst* did not age as quickly as *Δtpst* under control conditions (Fig. 4C). *Δtpst* grown on either PpPSY1 or AtPSY1 did not senesce at the same time as *Δtpst* under control conditions. Therefore, supplementing media with exogenous PSY1 can rescue all developmental aspects of the *Δtpst* phenotype, restoring normal protonemal growth, gametophore development, and timing of senescence, although a higher concentration of PpPSY1 was required. Notably, the ability of AtPSY1 to rescue *Δtpst* in *P. patens* suggests that the PSY signaling pathway is evolutionarily conserved.

Given that Arabidopsis PSY1 peptide influences *P. patens* development, we tested whether PSY from *P. patens* affects other plant species. Previous work demonstrated that exogenous application of PSY peptides promotes root growth in Arabidopsis and rice (Pruitt *et al.*, 2017; Ercoli *et al.*, 2024; Shi *et al.*, 2024), so we conducted root assays in these species using the synthetic PpPSY1 peptide. In Arabidopsis, we were able to confirm that both wild-type and *tpst-1* plants showed a root elongation phenotype in response to PpPSY1 treatment, similar to that of AtPSY1, when compared to mock-treated plants (Fig. 5 A,B). Additionally, exogenous application of PpPSY1 peptide promoted root elongation in wild-type Kitaake seedlings (Fig. 5C, D). These results further support that PSY signaling is evolutionarily conserved.

Discussion

Here, we report that sulfotyrosyl peptides are critical for cellular expansion, as Pp*tpst* null mutants (*Δtpst*), which are deficient in producing sulfated peptides, have

197 defects in cell expansion in the juvenile (protonemata) and adult (gametophores) phases of
198 moss growth, and age earlier than wild-type plants. All the *Δtpst* developmental
199 phenotypes in *P. patens* were rescued by exogenous application of AtPSY1. Reciprocally,
200 exogenous addition of PpPSY1 to both Arabidopsis and rice elicited root elongation. These
201 results indicate that PSY peptides act as functional orthologs in plant development and
202 further suggest that peptide recognition may function through an evolutionarily conserved
203 signaling pathway. While PSY receptors have been identified and characterized in
204 Arabidopsis (Ogawa-Ohnishi *et al.*, 2022), future work will aim to elucidate the receptors in
205 *P. patens* and their downstream signaling modules. The comparison of peptide function in
206 different plant species and the binding of orthologous receptors will shed light on the
207 conserved biological functions mediated by PSY-signaling.

208 Overall, our findings indicate that PSY signaling is conserved in *P. patens* and is
209 critical for development. Null mutants of *TPST* in both Arabidopsis and *P. patens* have a
210 similar phenotype, generally characterized by smaller plant size, which indicates functional
211 conservation of TPST. The lower efficacy of PpPSY1 in rescuing *Δtpst* might be attributed to
212 the PpPSY1 peptide sequence containing two cysteine residues, giving the synthesized
213 peptide the potential to be easily oxidized over time, and therefore, it might not be active
214 long-term in the media. The inability of AtPSK1 to rescue *Δtpst* might be explained by the
215 possibility that PSK1 is not sulfated in *P. patens*. The putative PSK1 sequence from *P.*
216 *patens* (Furumizu *et al.*, 2021) lacks the highly conserved aspartic acid residue that
217 precedes the PSK1 peptide sequence. All known sulfated peptides, with the exception of
218 GLV9, contain a DY motif (Kaufmann and Sauter, 2019), which is absent from the PSK1
219 sequence in *P. patens*. The aspartic acid residue that precedes the sulfated tyrosine
220 residue is one of the most important factors for directing tyrosine sulfation in PSK1
221 (Matsubayashi and Sakagami, 1996). Given the absence of this motif from PpPSK1, which
222 instead has an FY motif, it is possible that the mature peptide lacks a sulfated tyrosine,
223 suggesting that PSK signaling in *P. patens* does not require tyrosine sulfation.

224 Recently, two immune-responsive small secreted peptides were identified in *P.*
225 *patens* as sharing similarities with the PSY peptide motif, creating a new category of

226 sulfated peptides, PSY-like (PSYL) (Lyapina *et al.*, 2025). Quantification of protonemal cell
227 elongation of wild-type plants on media containing varying concentrations of both the
228 sulfated and non-sulfated versions of PSY, PSYL1, and PSYL2 showed that the sulfation of
229 the tyrosine residue is necessary for activity of the PSY and PSYL peptides in *P. patens*. This
230 result is consistent with our finding that TPST function and, therefore, its post-translational
231 modification of sTyr peptides, were critical for proper development. The addition of
232 sulfated PSY, PSYL1, or PSYL2 to the media increases cell length, which is in line with our
233 findings that the addition of exogenous PSY increased plant growth. Both PSYL1 and PSYL2
234 peptide sequences contain a motif that resembles the PSY peptide motif
235 (DY*(D)(P)**N**H*P), but the conserved His and Pro residues are in different positions
236 than in PSY (Lyapina *et al.*, 2025). Given the resemblance to PSY, it is possible that the
237 addition of exogenous PSYL1 and PSYL2 could rescue some of the developmental deficits
238 of *Δtpst*, including protonemal plant size, gametophore expansion, and senescence.

239 Moss mutants carrying an alanine substitution of the candidate catalytic base, His-
240 124 in PpTPST, resembled the moss *Δtpst* mutant phenotype. This indicates that His-124 is
241 essential for protein function and thus necessary for proper plant development. These
242 observations agree with prior findings that the histidine in the active site of *M. musculus*
243 EST and *F. chlorifoli*a F3ST is required for enzymatic activity (Marsolais and Varin, 1997;
244 Kakuta *et al.*, 1998). Thus, the conserved histidine found in the active site of other studied
245 sulfotransferases, which is required for catalytic activity, is conserved in plant TPSTs.
246 Based on this finding and the identification of putative PAPs-binding motifs in plant TPSTs
247 (Stewart and Ronald, 2022), it is possible that plant and animal TPSTs did not evolve via
248 convergent evolution as first suggested (Komori *et al.*, 2009).

249 Although *tpst-H124A* most closely resembled *Δtpst*, the other point mutants, *tpst-*
250 *R81A,* and *tpst-R144A*, are the same size as *Δtpst*, but with a lower circularity, which could
251 potentially be attributed to the point mutants retaining some weak PAPS binding. Prior
252 studies have found that some missense substitutions in the 5'-PSB and 3'-PSB motifs of
253 other sulfotransferases retain some wild-type enzymatic activity (Bick *et al.*, 2010; Liu and
254 Pedersen, 2022). Therefore, this residual activity could help explain the small protonemal

255 phenotype of *tpst-R81A* and *tpst-R144A,* as well as the variability in gametophore formation
256 between plants. This finding suggests that plant TPSTs use the same catalytic mechanism
257 as animal sulfotransferases.

258

259 **Materials and Methods**

260 *Tissue propagation*

261 *P. patens* lines were propagated weekly by moderate homogenization in water and
262 then plated onto PpNH4 (1.03 mM MgSO4, 1.86 mM KH_2PO_4, 3.3 mM $Ca(NO_3)_2$, 2.7 mM
263 $(NH_4)_2$-tartrate, 45 μM $FeSO_4$, 9.93 μM H_3BO_3, 220 nM $CuSO_4$, 1.966 μM $MnCl_2$, 231 nM
264 $CoCl_2$, 191 nM $ZnSO_4$, 169 nM KI, and 103 nM Na_2MoO_4, containing 0.7% agar) plates
265 covered with cellophane (Wu and Bezanilla, 2014). Tissue was grown in Percival growth
266 chambers at room temperature under 85 $\mu mol_{photons}/m^2s$ light with long-day (16/8)
267 conditions. Peptide media was created by pouring 25 mL PpNH4 plates supplemented with
268 either 200 nm AtPSY1, 200nM AtPSK1, or 1 μM PpPSY1.

269

270 *RT-PCR*

271 We isolated total RNA from 8-day old wild-type plants regenerated from protoplasts
272 using an RNeasy Plant mini prep kit (Qiagen). cDNA was prepared from 1μg of total RNA
273 using a SuperScript III reverse transcriptase kit, following the manufacturer's
274 recommendation (Invitrogen). We amplified the TPST transcripts using the primers listed in
275 Supplementary Table 2 using 1 μL of cDNA.

276

277 *Generation of knockout and point mutation lines*

278 Approximately one-week-old tissue was used for transformations. Transformations
279 into *P. patens* protoplasts were done using the PEG-mediated transformation protocol

280 described in (Wu, Ryken and Bezanilla, 2023). To generate knockouts (*Δtpst-6)*, 15 µg of the
281 CRISPR plasmid (pMH-Cas9-sgRNA plasmid backbone) was used. For HDR
282 transformations using annealed oligonucleotides (*Δtpst-7, tpst-R81A, tpst-H124A, tpst-*
283 *R144A*), 15 µg of the CRISPR plasmid and 10 µL of annealed oligonucleotides were used.
284 The sequences of each oligonucleotide and protospacer used are located in
285 Supplementary Table 2.

286 After transformation, protoplasts were plated onto PRMB media covered in
287 cellophane and left to recover for 4 days. The cellophane from the PRMB media (PpNH4
288 medium supplemented with 8.5% mannitol and 10 mM $CaCl_2$), which contains the
289 protoplasts, was moved to selection (PpNH4 media containing 15 µg ml^{-1} hygromycin) for 1
290 week. Surviving protoplasts have taken up the CRISPR plasmid. After 1 week of selection,
291 the cellophane was moved to PpNH4 media. After 1-2 weeks, protoplast-regenerated
292 plants were individually picked to fresh PpNH4 plates without cellophane, before being
293 genotyped around 2 weeks later.

294

295 *Genotyping*

296 Genomic DNA was extracted from *P. patens* tissue (Wu, Ryken and Bezanilla, 2023).
297 Competition PCR was used to genotype plants. All genotyping primers are listed in
298 Supplementary Table 2. Competition PCR uses two primers, one forward and one reverse,
299 that are around 500 base pairs upstream and downstream of the protospacer region. In
300 addition, a third internal primer was used, which was designed to anneal to the CRISPR cut
301 site. Therefore, in edited plants, the internal primer does not bind, and only the larger PCR
302 product is obtained. If the plant is not edited, the shorter PCR product, using the internal
303 primer, is preferentially produced. Any plants that had a larger PCR product were used to
304 PCR amplify the targeted region a second time, using only the external primers. The PCR
305 product was sequenced using Sanger sequencing.

306 To identify point mutations, a second competition PCR was conducted using the
307 same external primers and one primer that annealed to the desired point mutation and
308 silent mutations. Therefore, in plants with the correct point mutation, the internal primer
309 binds, forming the smaller PCR product. Any plants without the correct point mutation had
310 a larger PCR product, as the internal primer could not bind. DNA from plants producing the
311 smaller product was then amplified again with the only external primers, and those
312 products were sequenced using Sanger sequencing.

313

314 *Imaging and morphometric analysis of growth assays*

315 Protoplast preparation for growth assays was performed using a standard protocol
316 (Wu, Ryken and Bezanilla, 2023). Approximately one week old ground tissue was
317 protoplasted and plated onto PRMB media for 4 days. Afterwards, the protoplasts on
318 cellophane were moved to PpNH4 media. All growth assays were performed using 2-week-
319 old plants except for the data presented in Fig. 4.

320 Brightfield and chlorophyll autofluorescence images were collected using a
321 stereomicroscope (Nikon SMZ25) equipped with a CCD color camera (Nikon digital DS-Fi2)
322 with a 1X objective. Acquisition settings were held at the same settings for each image.
323 Chlorophyll autofluorescence was captured using a 480/40 excitation filter with a 510 long
324 pass emission filter. The red channel of the fluorescence image corresponds to chloroplast
325 autofluorescence.

326 To ensure image acquisition occurred with the sample identity blinded to the
327 observer, the genotype of each line was hidden at the time of imaging. Each line was
328 imaged on the same day, and 30 images of individual plants were taken from each line.
329 Both brightfield and fluorescence images were collected. To quantify plant area, the red
330 channel was separated from each RGB fluorescence image. Images from the red channel
331 were then analyzed using a macro in ImageJ (Galotto, Bibeau and Vidali, 2019). The

threshold was set at max entropy and was manually set for each plant. The total area of each plant was calculated using the largest thresholded object in a cropped window.

For growth assays pertaining to plants grown on peptide, 1-week-old protoplasts on cellophane were transferred to peptide media or a fresh plate of PpNH4 as the control. After 5 days on peptide, 12-day-old protoplast-regenerated plants were imaged for growth assays. Growth assays were analyzed as described above. The cellophanes containing the protoplast-regenerated plants were moved to freshly poured peptide media or PpNH4 for the control on a weekly basis. Plants were moved to fresh media each week until senescence occurred.

Senescence

To check whether mutant plants have a senescence phenotype, individual plants from protoplast-regenerated tissue were placed on the same plate of PpNH4 and left in the growth chamber for several weeks until at least one line turned brown (senescence). Senescence images were taken using a cellphone.

Peptide Synthesis

The peptides used in this study include PpPSY1 (DY^{S}EKPCANKKHDPSVCKNG), AtPSY1 (DY^{S}GDPSANPKHDPGVPPSA) and AtPSK1 (Y^{S}IY^{S}TQ). All peptides are tyrosine-sulfated as indicated (Y^{S}). The synthetic AtPSY1 peptide used in these experiments lacks the hydroxy- and L-Ara3- modifications at the C-terminus. All peptides were obtained from Pacific Immunology (Ramona, CA, USA) and resuspended in double distilled water.

Root Growth Assays

356 *Arabidopsis thaliana* ecotype Columbia (Col-0, wild type) and *tpst-1* (SALK_009847)
357 seeds were surface sterilized with 70% ethanol for 10 minutes, rinsed three times with
358 100% ethanol, and then stratified in 0.1% agarose for 2-4 days at 4°C before germination.
359 Seedlings were sown on standard 1X MS media plates (Murashige Skoog salt mixture with
360 vitamins, MSP09-Caisson Laboratories), 1% sucrose, and 0.3% gellan gum (G024-Caisson-
361 Gelzan), adjusted to pH 5.8 with KOH. MS plates were supplemented with various
362 concentrations of synthetic PpPSY1, AtPSY1, or water (mock control). For each experiment,
363 MS media was freshly prepared and cooled in a 55-60°C water bath after autoclaving
364 before adding chemicals. Seeds were placed on the plates (15-20 seeds per plate) and the
365 lids were secured with Micropore surgical tape (1530-0). For root assays, plants were grown
366 in vertically positioned plates in a chamber under long day conditions (16 hours light:8
367 hours dark) at 21°C. Germination for each seedling was marked, and primary root length
368 was marked every day until the end of the experiment (6-or 8-days post germination, dpg).
369 Arabidopsis root plates were scanned and primary root growth was measured using Fiji Is
370 Just ImageJ (Version 2.16) (Schindelin *et al.*, 2012).

371 *Oryza sativa* ssp. *Japonica* cultivar Kitaake (wild type) seeds were dehusked,
372 surface-sterilized in 20% bleach for 30 minutes, and thoroughly washed with autoclaved
373 water. The seeds were grown on 1X MS media (MSP09-Caisson Laboratories) with 1%
374 sucrose (pH 5.8), either as solid media plates containing 0.3% gellan gum or
375 hydroponically in flasks with 100 mL of 1X MS without gellan gum. For solid medium
376 conditions, seeds were sown on plates (15 per plate), sealed with Micropore tape, and
377 placed vertically for 7 days. For hydroponic conditions, flasks containing 1X MS were
378 cooled before adding peptides and sterilized seeds (15 per flask), and then placed in the
379 rice incubator for 6 days. The incubators used for rice germination and growth were set
380 with a 14-h-light/10-h-dark photoperiod at 28°C/24°C. MS plates or flasks were
381 supplemented with synthetic PpPSY1 or water (mock control), the concentration of the
382 peptide treatment is specified in the figure legends. For rice seedlings grown on plates, the
383 germination was marked and the root length was marked every day until the end of the
384 experiment (6 dpg). Rice seedlings grown hydroponically or on solid media were imaged

and root length measurements were done in Fiji Is Just ImageJ (Version 2.16) (Schindelin *et al.*, 2012).

Statistical Analyses

A non-parametric approach was taken to analyze differences between different experimental groups. Statistical significance was determined using a Kruskal-Wallis test followed by a post-hoc Dunn's test when a significant difference was found. A Bonferroni correction was applied to the p-values resulting from Dunn's test to control for multiple comparisons. Pairwise adjusted p-values at a significance level of $\alpha = 0.05$ were used to identify groups that were statistically different from each other. The compact letter display (CLD) approach was used to categorize each group into statistically distinguishable subsets. Letters were assigned to indicate significance between groups. Groups with the same letter were not statistically different. Groups with non-overlapping letters are not statistically different. Analyses were performed using R version 4.4.1 (Team, R. C., 2024).

Acknowledgements

We thank Maria Florencia Ercoli for the Arabidopsis *tpst-1* seeds and for advice on this manuscript and Valley Stewart for helpful discussions. This work was funded by the following grants: National Science Foundation (IOS-2436798) to MB and (IOS-1954929) to PCR, National Institute of Health (R35 GM148173) to PCR, USDA-NIFA-AFRI Postdoctoral Fellowship (2023-67012-39889) to AMS, and Dartmouth Undergraduate Research (Barbara E. Crute Memorial Internship) to DVT.

References

Amano, Y. *et al.* (2007) "Tyrosine-sulfated glycopeptide involved in cellular proliferation and expansion in Arabidopsis," *Proceedings of the National Academy of Sciences*, 104(46), pp. 18333–18338. Available at: https://doi.org/10.1073/pnas.0706403104.

Bick, M.J. *et al.* (2010) “Crystal Structures of the Glycopeptide Sulfotransferase Teg12 in a Complex with the Teicoplanin Aglycone,” *Biochemistry*, 49(19), pp. 4159–4168. Available at: https://doi.org/10.1021/bi100150v.

Cosgrove, D.J. (2005) “Growth of the plant cell wall,” *Nature Reviews Molecular Cell Biology*, 6(11), pp. 850–861. Available at: https://doi.org/10.1038/nrm1746.

Doblas, V.G. *et al.* (2017) “Root diffusion barrier control by a vasculature-derived peptide binding to the SGN3 receptor,” *Science*, 355(6322), pp. 280–284. Available at: https://doi.org/10.1126/science.aaj1562.

Ercoli, M.F. *et al.* (2024) “Tyrosine-sulfated peptide hormone induces flavonol biosynthesis to control elongation and differentiation in Arabidopsis primary root.” bioRxiv, p. 2024.02.02.578681. Available at: https://doi.org/10.1101/2024.02.02.578681.

Furumizu, C. *et al.* (2021) “The sequenced genomes of nonflowering land plants reveal the innovative evolutionary history of peptide signaling,” *The Plant Cell*, 33(9), pp. 2915–2934. Available at: https://doi.org/10.1093/plcell/koab173.

Galotto, G., Bibeau, J.P. and Vidali, L. (2019) “Automated Image Acquisition and Morphological Analysis of Cell Growth Mutants in Physcomitrella patens,” in F. Cvrčková and V. Žárský (eds.) *Plant Cell Morphogenesis*. New York, NY: Springer New York (Methods in Molecular Biology), pp. 307–322. Available at: https://doi.org/10.1007/978-1-4939-9469-4_20.

Goodstein, D.M. *et al.* (2012) “Phytozome: a comparative platform for green plant genomics,” *Nucleic Acids Research*, 40(D1), pp. D1178–D1186. Available at: https://doi.org/10.1093/nar/gkr944.

Kakuta, Y. *et al.* (1998) “Conserved structural motifs in the sulfotransferase family,” *Trends in Biochemical Sciences*, 23(4), pp. 129–130. Available at: https://doi.org/10.1016/S0968-0004(98)01182-7.

Kaufmann, C. and Sauter, M. (2019) “Sulfated plant peptide hormones,” *Journal of Experimental Botany*, 70(16), pp. 4267–4277. Available at: https://doi.org/10.1093/jxb/erz292.

Komori, R. *et al.* (2009) “Identification of tyrosylprotein sulfotransferase in Arabidopsis,” *Proceedings of the National Academy of Sciences*, 106(35), pp. 15067–15072. Available at: https://doi.org/10.1073/pnas.0902801106.

Liu, J. and Pedersen, L.C. (2022) “Emerging chemical and biochemical tools for studying 3-O-sulfated heparan sulfate,” *American Journal of Physiology-Cell Physiology*, 322(6), pp. C1166–C1175. Available at: https://doi.org/10.1152/ajpcell.00110.2022.

Lyapina, I. *et al.* (2025) “Comparative analysis of small secreted peptide signaling during defense response: insights from vascular and non-vascular plants,” *Physiologia Plantarum*, 177(2), p. e70147. Available at: https://doi.org/10.1111/ppl.70147.

Marsolais, F. and Varin, L. (1997) “Mutational Analysis of Domain II of Flavonol 3-Sulfotransferase,” *European Journal of Biochemistry*, 247(3), pp. 1056–1062. Available at: https://doi.org/10.1111/j.1432-1033.1997.01056.x.

Matsubayashi, Y. *et al.* (1999) “Physiological relationships between auxin, cytokinin, and a peptide growth factor, phytosulfokine-α, in stimulation of asparagus cell proliferation,” *Planta*, 207(4), pp. 559–565. Available at: https://doi.org/10.1007/s004250050518.

Matsubayashi, Y. and Sakagami, Y. (1996) “Phytosulfokine, sulfated peptides that induce the proliferation of single mesophyll cells of Asparagus officinalis L.,” *Proceedings of the National Academy of Sciences*, 93(15), pp. 7623–7627. Available at: https://doi.org/10.1073/pnas.93.15.7623.

Matsuzaki, Y. *et al.* (2010) “Secreted Peptide Signals Required for Maintenance of Root Stem Cell Niche in Arabidopsis,” *Science*, 329(5995), pp. 1065–1067. Available at: https://doi.org/10.1126/science.1191132.

Nakayama, T. *et al.* (2017) “A peptide hormone required for Casparian strip diffusion barrier formation in Arabidopsis roots,” *Science*, 355(6322), pp. 284–286. Available at: https://doi.org/10.1126/science.aai9057.

Ogawa-Ohnishi, M. *et al.* (2022) “Peptide ligand-mediated trade-off between plant growth and stress response,” *Science*, 378(6616), pp. 175–180. Available at: https://doi.org/10.1126/science.abq5735.

Pruitt, R.N. *et al.* (2017) “A microbially derived tyrosine-sulfated peptide mimics a plant peptide hormone,” *New Phytologist*, 215(2), pp. 725–736. Available at: https://doi.org/10.1111/nph.14609.

Rensing, S.A. *et al.* (2020) “The Moss Physcomitrium (Physcomitrella) patens: A Model Organism for Non-Seed Plants[OPEN],” *The Plant Cell*, 32(5), pp. 1361–1376. Available at: https://doi.org/10.1105/tpc.19.00828.

Schindelin, J. *et al.* (2012) “Fiji: an open-source platform for biological-image analysis,” *Nature Methods*, 9(7), pp. 676–682. Available at: https://doi.org/10.1038/nmeth.2019.

Schumaker, K.S. and Dietrich, M.A. (1998) “HORMONE-INDUCED SIGNALING DURING MOSS DEVELOPMENT,” *Annual Review of Plant Biology*, 49(Volume 49, 1998), pp. 501–523. Available at: https://doi.org/10.1146/annurev.arplant.49.1.501.

Shi, L.-D. *et al.* (2024) “Reduced methane emissions in transgenic rice genotypes are associated with altered rhizosphere microbial hydrogen cycling.” bioRxiv, p. 2024.10.07.617079. Available at: https://doi.org/10.1101/2024.10.07.617079.

Stewart, V. and Ronald, P.C. (2022) “Sulfotyrosine residues: Interaction specificity determinants for extracellular protein–protein interactions,” *Journal of Biological Chemistry*, 298(8), p. 102232. Available at: https://doi.org/10.1016/j.jbc.2022.102232.

Team, R. C. (2024) “R: A Language and Environment for Statistical Computing, version 4.4.1.” Available at: www.R-project.org.

The UniProt Consortium (2025) “UniProt: the Universal Protein Knowledgebase in 2025,” *Nucleic Acids Research*, 53(D1), pp. D609–D617. Available at: https://doi.org/10.1093/nar/gkae1010.

Wu, S.-Z. and Bezanilla, M. (2014) “Myosin VIII associates with microtubule ends and together with actin plays a role in guiding plant cell division,” *eLife*. Edited by D.C. Bergmann, 3, p. e03498. Available at: https://doi.org/10.7554/eLife.03498.

Wu, S.-Z., Ryken, S.E. and Bezanilla, M. (2023) “CRISPR-Cas9 Genome Editing in the Moss Physcomitrium (Formerly Physcomitrella) patens,” *Current Protocols*, 3(4), p. e725. Available at: https://doi.org/10.1002/cpz1.725.

Zhao, C. *et al.* (2019) “Evolution of chloroplast retrograde signaling facilitates green plant adaptation to land,” *Proceedings of the National Academy of Sciences*, 116(11), pp. 5015–5020. Available at: https://doi.org/10.1073/pnas.1812092116.

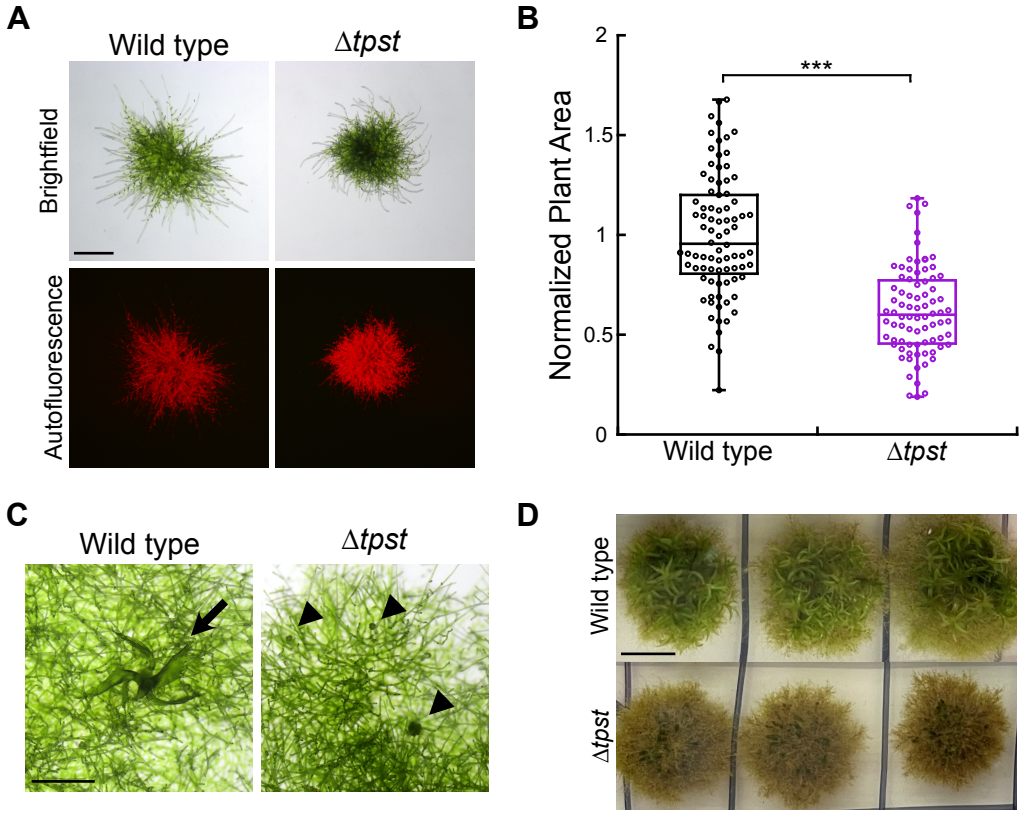

Figure 1. TPST is required for normal development. A) Representative brightfield and chlorophyll autofluorescence images of 2-week-old wild type and Δ*tpst* from plants that were regenerated from protoplasts. Scale, 500 µm. B) Plant area was quantified and normalized to wild type. Significance was calculated using a Kruskal-Wallis Test with a significance level of $\alpha=0.05$. $p<0.0001$. Experiments repeated three independent times. C) Representative brightfield images of 5-week-old tissue that had been regenerated from protoplasts. Arrow denotes a fully expanded gametophore. Arrowheads denote gametophore buds. Scale, 500 µm. D) 11-week-old whole plants that were regenerated from protoplasts. Scale, 0.5 cm.

A

		5'-PSB motif		Catalytic base		3'-PB motif	
EST	47..	PKAGTTWI	53	H	17	IYLCRNAKDVAVSYYY	..141
HS3OST-1	63..	PKGGTRAL	15	E	55	LLILRDPSERVLSDYT	..158
HS2OST	82..	PKTASTSF	50	H	17	INVIRDPIERLVSYYY	..175
HS6OST-3	103..	QKTGGTTF	47	H	28	ITMLRDPVSRYLSEWK	..202
Animal TPST	78..	PRSGTTLM	14	E	79	LLMVRDGRASVHSMIS	..195
Bacterial TPST	10..	PRAGSSLL	8	H	77	ICCVRDVGWIVDSFER	..121
A. thaliana TPST	66..	PRTGGRTY	36	H	16	MTIVRDPIARVLSTYE	..142
P. patens TPST	80..	PRTGGRTY	36	H	15	VTNLRNPVNRVLSTYE	..155
		81		124		144	

B

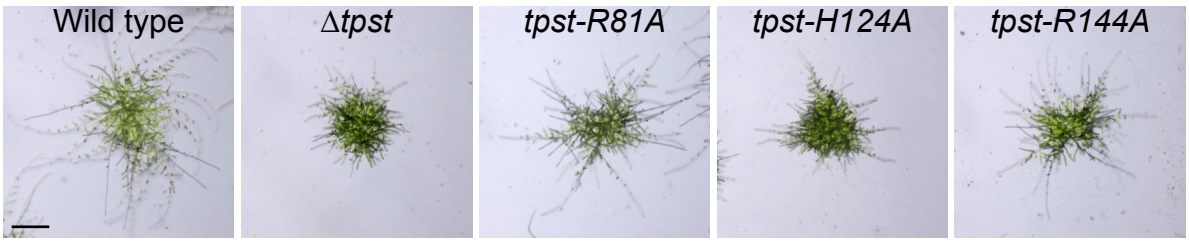

C

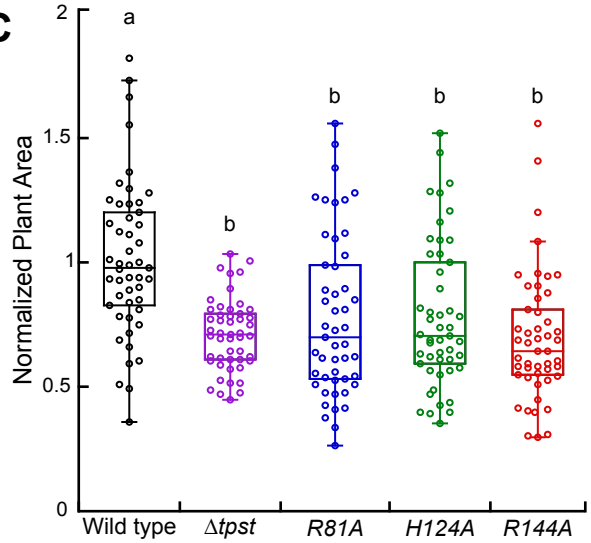

D

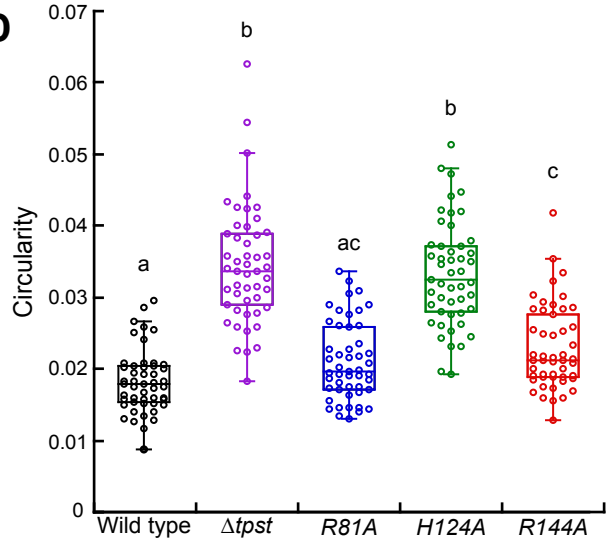

E

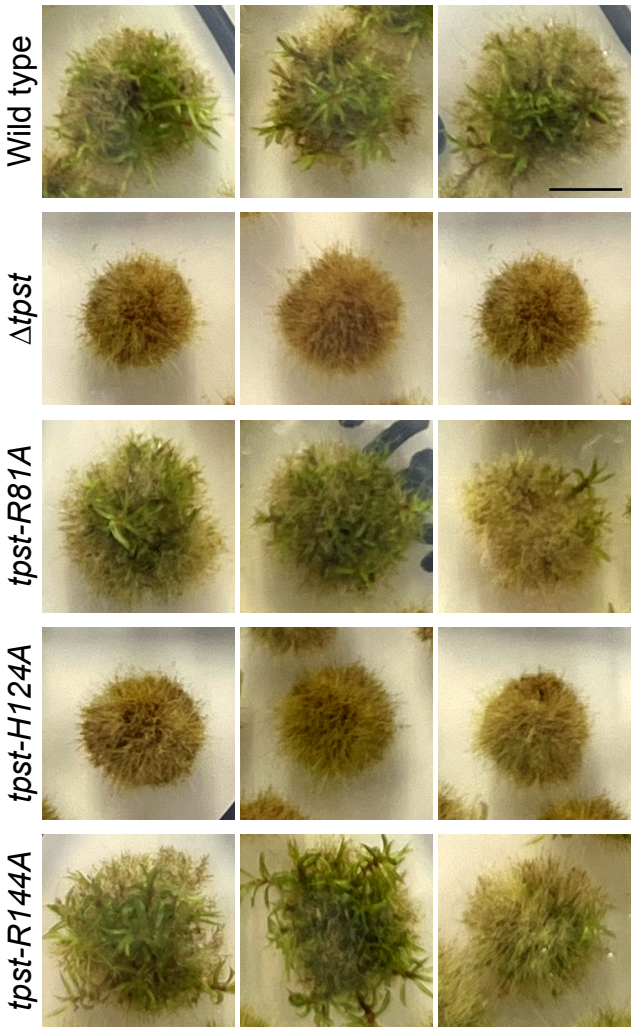

Figure 2. Histidine 124 is catalytically important for TPST function. A) Sequence motifs of different sulfotransferases across organisms showing the 5'-PSB, candidate catalytic base, and 3'-PB. Adapted from Stewart and Ronald, 2022 to include *P. patens* TPST. Numbers on the left and right of the motifs indicate the starting and ending position. The numbers between motifs indicate the number of residues in between the selected sequences. Substitutions of residues in red decrease enzymatic activity. Numbers underneath the black boxes indicate the position in *P. patens* TPST. Enzymes are EST, estrogen 17-β sulfotransferase (*Mus musculus*; Protein Data Bank [PDB] code: 1AQU); HS3OST-1, heparan sulfate (3-O) sulfotransferase (*M. musculus*; PDB code: 1S6T); HS2OST, heparan sulfate (2-O) sulfotransferase (*Homo sapiens*; PDB code: 3F5F); HS6OST-3, heparan sulfate (6-O) sulfotransferase (*Danio rerio*; PDB code: 5T03); animal TPST (*H. sapiens*; PDB code: 5WRI); bacterial TPST (*Xanthomonas spp*.; GenBank accession number: WP_027703307); *A. thaliana* TPST (*Arabidopsis thaliana*; BAI22702); *P. patens* TPST (NCBI Reference Sequence: XM_ 024542583.2). B) Representative brightfield images of 2-week-old plants regenerated from protoplasts. Scale represents 500 µm. C and D) Quantification of plant area and circularity using images of 2-week-old regenerated protoplasts. Plant area is quantified and normalized to wild type. Significance was calculated using a Kruskal-Wallis Test with a significance level of $\alpha=0.05$. Experiments repeated three independent times. E) 8-week-old whole plants from protoplast-regenerated tissue. Scale represents 0.5 cm.

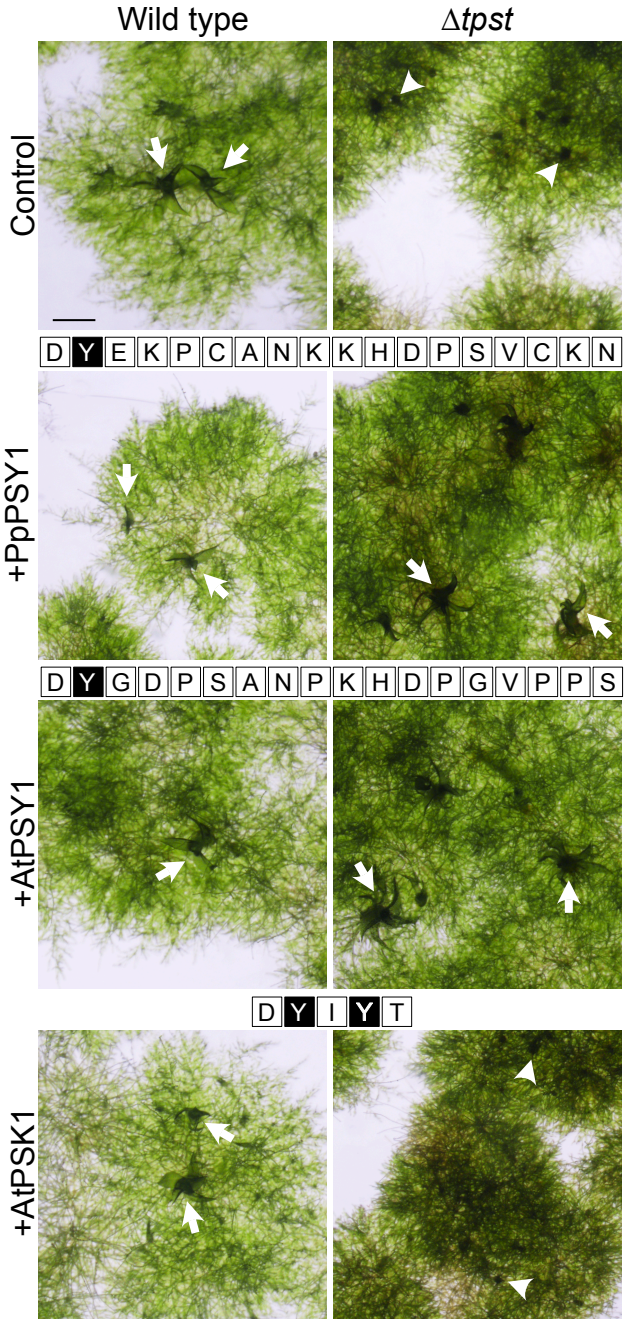

Figure 3. Addition of exogenous PSY1 induces gametophore expansion in Δ*tpst*. 20-day-old protoplast-regenerated plants after 12 days on PpNH4 media supplemented with either 1 µm PpPSY1, 200 nM AtPSY1, or 200 nM AtPSK1. Arrows denote an example of a fully expanded gametophore. Arrowheads denote an example of a gametophore bud. The 18 amino acid sequence of PSY1 in *P. patens* (moss) and *A. thaliana,* and the 5 amino acid sequence of PSK1 in *A. thaliana* are shown above the corresponding image. Black boxes represent the sulfated tyrosine residues. Scale bar represents 0.1 cm.

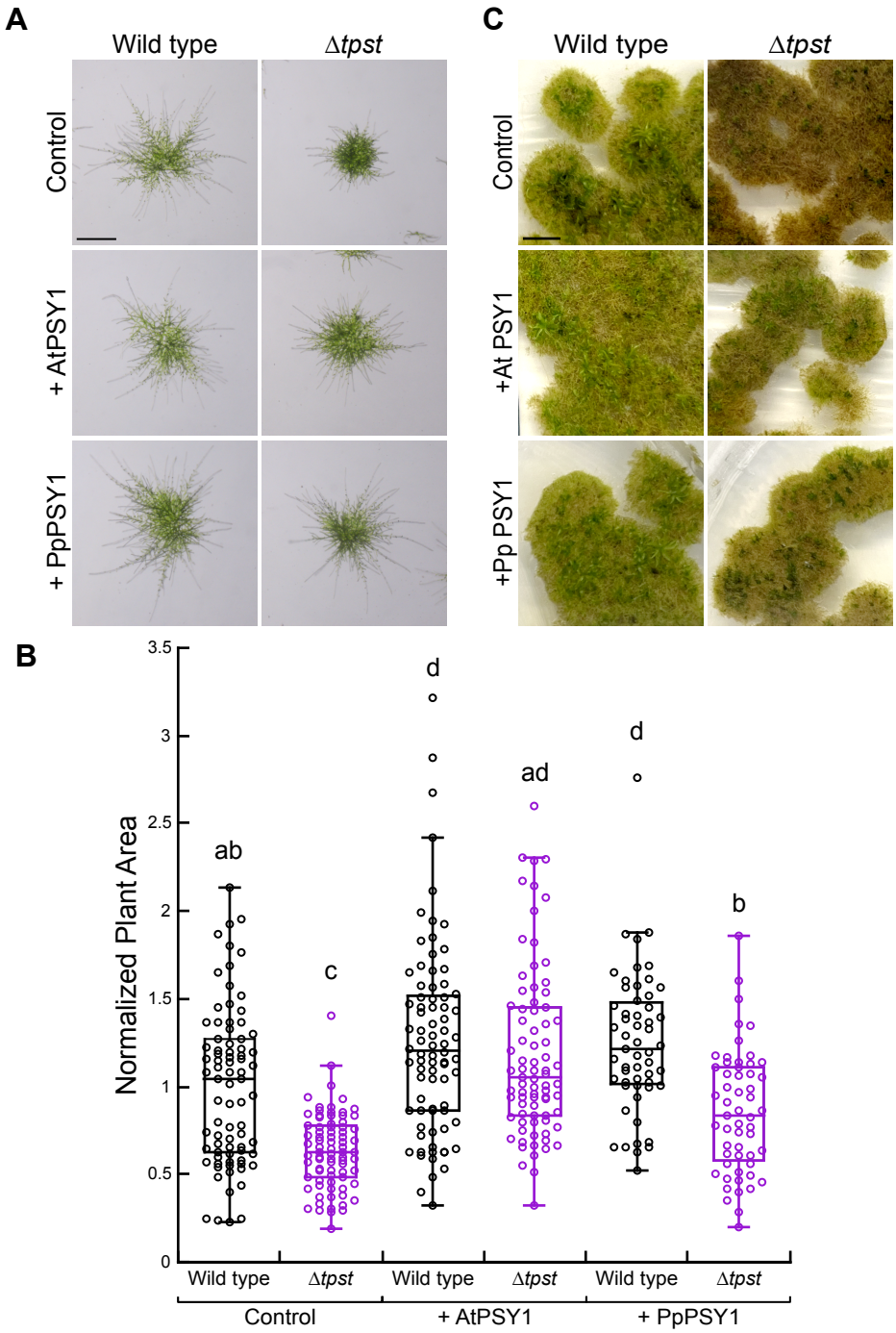

Figure 4. Exogenous PSY1 enhances growth. A) Representative brightfield images of wild type and Δ*tpst* from 12-day-old regenerated protoplasts. Scale represents 500 µm. B) Quantification of plant area using images of 12-day-old regenerated protoplasts. Plant area is quantified and normalized to the wild-type control. Letters indicate groups that are significantly different as determined by a Kruskal-Wallis test ($\alpha = 0.05$) with a Dunn's post hoc test and Bonferroni correction. Experiments repeated three independent times. C) 7-week-old whole plants from protoplast-regenerated tissue. Scale represents 0.5 cm.

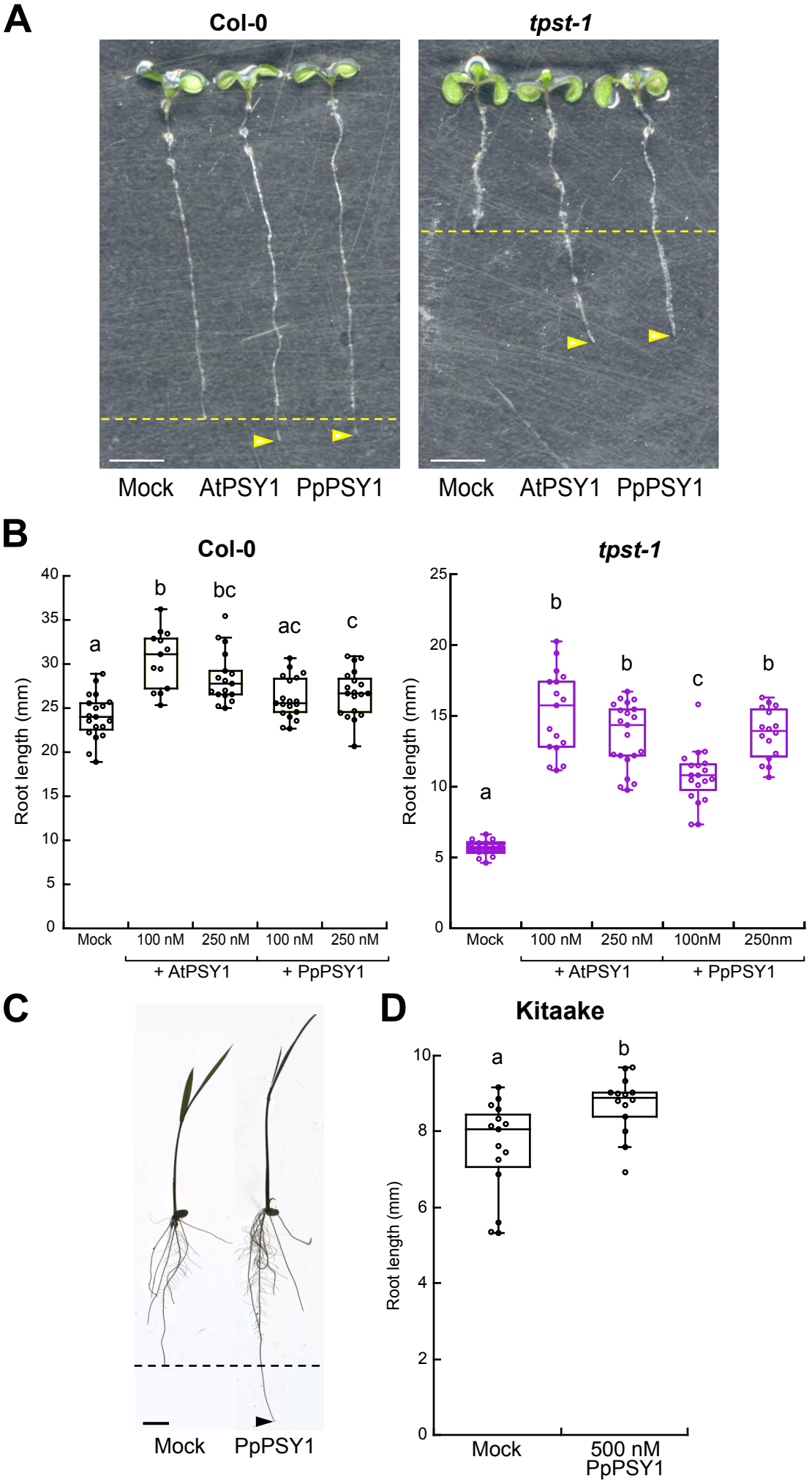
A
Col-0
tpst-1
Mock
AtPSY1
PpPSY1
Mock
AtPSY1
PpPSY1
B
Col-0
tpst-1
Root length (mm)
Mock
100 nM
250 nM
100 nM
250 nM
+ AtPSY1
+ PpPSY1
Mock
100 nM
250 nM
100nM
250nm
+ AtPSY1
+ PpPSY1
C
Mock
PpPSY1
D
Kitaake
Root length (mm)
Mock
500 nM
PpPSY1

Figure 5: Synthetic PpPSY1 peptide promotes root elongation in Arabidopsis & Rice seedlings. (A) Representative images of primary root growth of Col-0 (wild type, left) or *tpst-1* (right) seedlings 6-days-post germination (dpg) grown on 1X MS vertical plates with or without synthetic peptide treatment (250nM AtPSY1 or PpPSY1). Enhanced root elongation of peptide treated samples indicated by the white serrated line, with the arrows indicating the primary root tip. Scale represents 5mm. (B) Quantification of primary root elongation for Col-0 (left) or *tpst-1* (right) seedlings (n= 13-20) grown on 1X MS vertical plates with or without synthetic peptide PpPSY1 or AtPSY1 treatment (100nM or 250nM). 6-dpg for Col-0 and 8-dpg for *tpst-1*. Different letters indicate significant differences, as determined by a Kruskal-Wallis test ($\alpha = 0.05$) with a Dunn's post hoc test and Bonferroni correction. Experiments repeated three independent times. (C) Representative image of primary root growth of Kitaake (wild type) seedlings grown hydroponically in 1X MS with or without synthetic PpPSY1 treatment (500nM), 6-days-post treatment. Enhanced root elongation of peptide treated samples indicated by the black serrated line, with the arrows indicating the primary root tip. Scale bar represents 1cm. (D) Quantification of root elongation of Kitaake seedlings (n= 14-15), 6-dpg, grown on 1X MS plates with or without synthetic 500nM PpPSY1 treatment. Different letters indicate significant differences, as determined by a Kruskal-Wallis test ($\alpha = 0.05$). Experiments repeated three independent times.

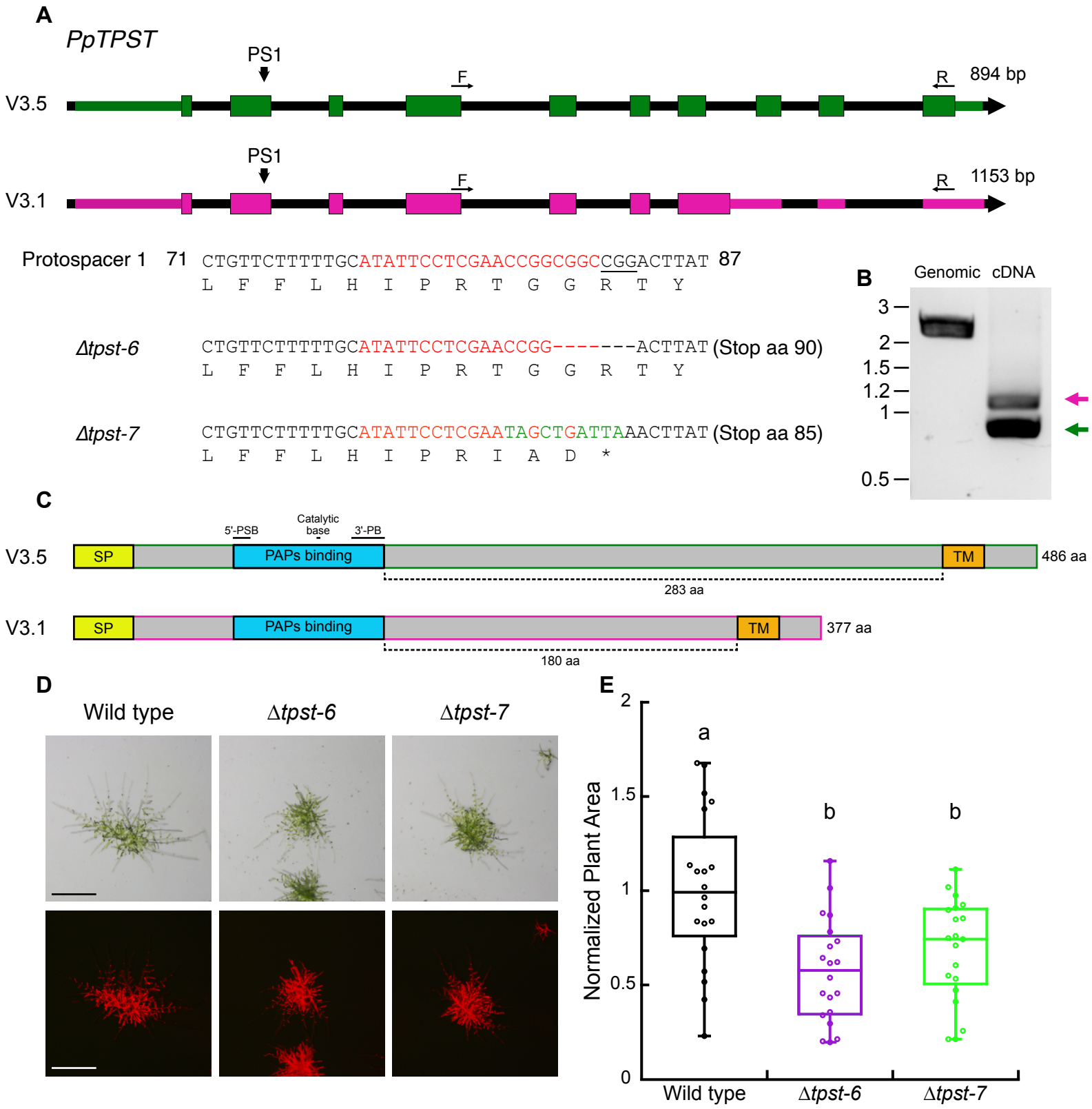
A
PpTPST
PS1
F
R
894 bp
V3.5
PS1
F
R
1153 bp
V3.1
Protospacer 1 71 CTGTTCTTTTTGCATATTCCTCGAACCGGCGGCCGGACTTAT 87
L F F L H I P R T G G R T Y
Δtpst-6 CTGTTCTTTTTGCATATTCCTCGAACCGG-------ACTTAT (Stop aa 90)
L F F L H I P R T G G R T Y
Δtpst-7 CTGTTCTTTTTGCATATTCCTCGAATAGCTGATTAAACTTAT (Stop aa 85)
L F F L H I P R I A D *
B
Genomic cDNA
3
2
1.5
1.2
1
0.5
C
5'-PSB
Catalytic base
3'-PB
V3.5
SP
PAPs binding
TM
486 aa
283 aa
V3.1
SP
PAPs binding
TM
377 aa
180 aa
D
Wild type
Δtpst-6
Δtpst-7
E
Normalized Plant Area
2
1.5
1
0.5
0
a
b
b
Wild type
Δtpst-6
Δtpst-7

Supplementary Figure 1. CRISPR-Cas9-mediated editing of *TPST*. A) Diagram of two predicted gene models of the *TPST* locus. Coding exons are represented by green (V3.5) or magenta (V3.1) boxes. Green lines represent the 5' and 3' UTR. Location of the protospacer targeted to create a *tpst* null mutant is denoted by PS1. The sequences below show the sequence around PS1, with the PS1 sequence in red. The PAM is underlined. All mutants have the indicated mutations, resulting in early translational stops. Deletions are indicated by dashes, and insertions are indicated in green text. Small arrows above each model indicate primers used for RT-PCR. Numbers on the right of each model indicate product size using cDNA. B) PCR products obtained with the indicated primers using either genomic DNA or cDNA isolated from protonemal tissue were separated on an agarose gel. Green arrow indicates the V3.5 transcript, and magenta arrow indicates the V3.1 transcript. C) TPST predicted primary structure encoded by the V3.5 or V3.1 transcript, drawn approximately to scale. SP denotes the signal peptide sequence. PAPs binding denotes the region between the first residue of the 5'-PSB motif and the last residue of the 3'-PB motif. Black lines indicate the approximate position of the 5'-PSB and 3'-PB elements, and the catalytic base. TM denotes the predicted transmembrane domain. The number of amino acids between the last residue of the 3'-PB and the first residue of the transmembrane domain is indicated below the dashed lines. D) Representative brightfield and chloroplast autofluorescence images of wild type, Δ*tpst-6*, and Δ*tpst-7* from 2-week-old plants that were regenerated from protoplasts. Scale, 500 μm. E) Plant area was quantified and normalized to wild type. Significant differences determined by a Kruskal-Wallis test ($\alpha = 0.05$) with a Dunn's post hoc test and Bonferroni correction are indicated by different letters.

```
Protospacer 1   74  CTGTTCTTTTTGCATATTCCTCGAACCGGCGGCCGGACTTAT  87
                    L  F  F  L  H  I  P  R  T  G  G  R  T  Y

tpst-R81A           CTGTTCTTTTTGCATATTCCTgctACtGGaGGaCGaACTTAT
                    L  F  F  L  H  I  P  A  T  G  G  R  T  Y

Protospacer 2  142  AATTTGCGCAACCCAGTGAATCGTGTGTTGAGCACCTATGAG  155
                    N  L  R  N  P  V  N  R  V  L  S  T  Y  E

tpst-R144A          AATTTGgctAAtCCtGTtAAcCGaGTGTTGAGCACCTATGAG
                    N  L  A  N  P  V  N  R  V  L  S  T  Y  E

Protospacer 3  115  CAGCCCAGCTGCAAGCTTTTGTCTTCACACGATGACATGAGC  128
                    Q  P  S  C  K  L  L  S  S  H  D  D  M  S

tpst-H124A          CAGCCtAGtTGtAAGCTTcTtTCaTCtgctGATGACATGAGC
                    Q  P  S  C  K  L  L  S  S  A  D  D  M  S
```

Supplementary Figure 2. Creating point mutations in *TPST*. Diagram of the *TPST* locus. Coding exons are represented by green boxes. Black lines represent the coding region, and green boxes represent the 5' and 3' UTR. Location of the protospacers used to create point mutations through HDR is denoted by PS1-3. The sequences below show the protospacer sequence in red, and the PAMs are underlined. Lowercase blue letters indicate base pair changes to incorporate silent mutations or alanine substitutions. Blue capital letters represent the point mutation.

499 **Figure legends**

500 **Figure 1. TPST is required for normal development.** A) Representative brightfield and
501 chlorophyll autofluorescence images of 2-week-old wild type and *Δtpst* from plants that
502 were regenerated from protoplasts. Scale, 500 µm. B) Plant area was quantified and
503 normalized to wild type. Significance was calculated using a Kruskal-Wallis Test with a
504 significance level of α=0.05. $p<0.0001$. Experiments repeated three independent times. C)
505 Representative brightfield images of 5-week-old tissue that had been regenerated from
506 protoplasts. Arrow denotes a fully expanded gametophore. Arrowheads denote
507 gametophore buds. Scale, 500 µm. D) 11-week-old whole plants that were regenerated
508 from protoplasts. Scale, 0.5 cm.

509

510 **Figure 2. Histidine 124 is catalytically important for TPST function.** A) Sequence motifs
511 of different sulfotransferases across organisms showing the 5'-PSB, candidate catalytic
512 base, and 3'-PB. Adapted from Stewart and Ronald, 2022 to include *P. patens* TPST.
513 Numbers on the left and right of the motifs indicate the starting and ending position. The
514 numbers between motifs indicate the number of residues in between the selected
515 sequences. Substitutions of residues in red decrease enzymatic activity. Numbers
516 underneath the black boxes indicate the position in *P. patens* TPST. Enzymes are EST,
517 estrogen 17-β sulfotransferase (*Mus musculus*; Protein Data Bank [PDB] code: 1AQU);
518 HS3OST-1, heparan sulfate (3-O) sulfotransferase (*M. musculus*; PDB code: 1S6T);
519 HS2OST, heparan sulfate (2-O) sulfotransferase (*Homo sapiens*; PDB code: 3F5F);
520 HS6OST-3, heparan sulfate (6-O) sulfotransferase (*Danio rerio*; PDB code: 5T03); animal
521 TPST (*H. sapiens*; PDB code: 5WRI); bacterial TPST (*Xanthomonas spp*.; GenBank
522 accession number: WP_027703307); *A. thaliana* TPST (*Arabidopsis thaliana*; BAI22702); *P.*
523 *patens* TPST (NCBI Reference Sequence: XM_024542583.2). B) Representative brightfield
524 images of 2-week-old plants regenerated from protoplasts. Scale represents 500 µm. C
525 and D) Quantification of plant area and circularity using images of 2-week-old regenerated
526 protoplasts. Plant area is quantified and normalized to wild type. Significance was
527 calculated using a Kruskal-Wallis Test with a significance level of α=0.05. Experiments

528 repeated three independent times. E) 8-week-old whole plants from protoplast-
529 regenerated tissue. Scale represents 0.5 cm.
530

531 **Figure 3. Addition of exogenous PSY1 induces gametophore expansion in *Δtpst*.** 20-
532 day-old protoplast-regenerated plants after 12 days on PpNH4 media supplemented with
533 either 1 µm PpPSY1, 200 nM AtPSY1, or 200 nM AtPSK1. Arrows denote an example of a
534 fully expanded gametophore. Arrowheads denote an example of a gametophore bud. The
535 18 amino acid sequence of PSY1 in *P. patens* (moss) and *A. thaliana,* and the 5 amino acid
536 sequence of PSK1 in *A. thaliana* are shown above the corresponding image. Black boxes
537 represent the sulfated tyrosine residues. Scale bar represents 0.1 cm.
538

539 **Figure 4. Exogenous PSY1 enhances growth.** A) Representative brightfield images of wild
540 type and *Δtpst* from 12-day-old regenerated protoplasts. Scale represents 500 µm. B)
541 Quantification of plant area using images of 12-day-old regenerated protoplasts. Plant
542 area is quantified and normalized to the wild-type control. Letters indicate groups that are
543 significantly different as determined by a Kruskal-Wallis test (α = 0.05) with a Dunn's post
544 hoc test and Bonferroni correction. Experiments repeated three independent times. C) 7-
545 week-old whole plants from protoplast-regenerated tissue. Scale represents 0.5 cm.
546

547 **Figure 5: Synthetic PpPSY1 peptide promotes root elongation in Arabidopsis & Rice**
548 **seedlings.** (A) Representative images of primary root growth of Col-0 (wild type, left) or
549 *tpst-1* (right) seedlings 6-days-post germination (dpg) grown on 1X MS vertical plates with
550 or without synthetic peptide treatment (250nM AtPSY1 or PpPSY1). Enhanced root
551 elongation of peptide treated samples indicated by the white serrated line, with the arrows
552 indicating the primary root tip. Scale represents 5mm. (B) Quantification of primary root
553 elongation for Col-0 (left) or *tpst-1* (right) seedlings (n= 13-20) grown on 1X MS vertical
554 plates with or without synthetic peptide PpPSY1 or AtPSY1 treatment (100nM or 250nM). 6-
555 dpg for Col-0 and 8-dpg for *tpst-1*. Different letters indicate significant differences, as
556 determined by a Kruskal-Wallis test (α = 0.05) with a Dunn's post hoc test and Bonferroni

557 correction. Experiments repeated three independent times. (C) Representative image of
558 primary root growth of Kitaake (wild type) seedlings grown hydroponically in 1X MS with or
559 without synthetic PpPSY1 treatment (500nM), 6-days-post treatment. Enhanced root
560 elongation of peptide treated samples indicated by the black serrated line, with the arrows
561 indicating the primary root tip. Scale bar represents 1cm. (D) Quantification of root
562 elongation of Kitaake seedlings (n= 14-15), 6-dpg, grown on 1X MS plates with or without
563 synthetic 500nM PpPSY1 treatment. Different letters indicate significant differences, as
564 determined by a Kruskal-Wallis test (α = 0.05). Experiments repeated three independent
565 times.

566

567 **Supplementary figure legends**

568 **Supplementary Figure 1. CRISPR-Cas9-mediated editing of *TPST*.** A) Diagram of two
569 predicted gene models of the *TPST* locus. Coding exons are represented by green (V3.5) or
570 magenta (V3.1) boxes. Green lines represent the 5' and 3' UTR. Location of the protospacer
571 targeted to create a *tpst* null mutant is denoted by PS1. The sequences below show the
572 sequence around PS1, with the PS1 sequence in red. The PAM is underlined. All mutants
573 have the indicated mutations, resulting in early translational stops. Deletions are indicated
574 by dashes, and insertions are indicated in green text. Small arrows above each model
575 indicate primers used for RT-PCR. Numbers on the right of each model indicate product
576 size using cDNA. B) PCR products obtained with the indicated primers using either
577 genomic DNA or cDNA isolated from protonemal tissue were separated on an agarose gel.
578 Green arrow indicates the V3.5 transcript, and magenta arrow indicates the V3.1
579 transcript. C) TPST predicted primary structure encoded by the V3.5 or V3.1 transcript,
580 drawn approximately to scale. SP denotes the signal peptide sequence. PAPs binding
581 denotes the region between the first residue of the 5'-PSB motif and the last residue of the
582 3'-PB motif. Black lines indicate the approximate position of the 5'-PSB and 3'-PB
583 elements, and the catalytic base. TM denotes the predicted transmembrane domain. The
584 number of amino acids between the last residue of the 3'-PB and the first residue of the

585 transmembrane domain is indicated below the dashed lines. D) Representative brightfield
586 and chloroplast autofluorescence images of wild type, *Δtpst-6*, and *Δtpst-7* from 2-week-
587 old plants that were regenerated from protoplasts. Scale, 500 µm. E) Plant area was
588 quantified and normalized to wild type. Significant differences determined by a Kruskal-
589 Wallis test (α = 0.05) with a Dunn's post hoc test and Bonferroni correction are indicated by
590 different letters.
591

592 **Supplementary Figure 2. Creating point mutations in *TPST*.** Diagram of the *TPST* locus.
593 Coding exons are represented by green boxes. Black lines represent the coding region, and
594 green boxes represent the 5' and 3' UTR. Location of the protospacers used to create point
595 mutations through HDR is denoted by PS1-3. The sequences below show the protospacer
596 sequence in red, and the PAMs are underlined. Lowercase blue letters indicate base pair
597 changes to incorporate silent mutations or alanine substitutions. Blue capital letters
598 represent the point mutation.
599

600 **Supplementary tables**

601 **Table S1.** Mutant lines used and created

Name	Background	Genetic alteration	Translation
Δ*tpst-6* (Δ*tpst*)	Wild type	7 bp deletion	Stop at AA90, aa 81-89 are irrelevant
Δ*tpst-7*	Wild type	Stop oligo insertion	Stop at AA85, aa 82-84 are irrelevant
tpst-R81A	Wild type	CGA→ GCT (241-243, AA change), C246T (silent), C249A (silent), C252A (silent)	R81A
tpst-H124A	Wild type	C348T (silent), C351T (silent), C354T (silent), T361C (silent), G363T (silent), T366A (silent), A369T (silent), CAC→ GCT (370-372, AA change)	H124A

tpst-R144A	Wild type	CGC→ GCT (430-432, AA change), C435T (silent), A438T (silent), G441T (silent), T444C (silent), T447A (silent)	R144A

Table S2. Table of primers, oligos, and protospacer sequences

Name	Sequence (5' to 3')	Purpose
TPST-F	AGCACACTTACTATCTGGCC	RT-PCR
TPST-R	gcccttgctcaccatcgatcctccgccaccCAGCTTTTCATGAACTTGCAAC	RT-PCR
TPST stop oligo F	ggaaaattctggaacttctgttctttttgcatattcctcgaaTAGCTGATTAAacttatcaccagtggtatggatttact	Stop oligo for TPST
TPST stop oligo R	agtaaatccataccactggtgataagtTTAATCAGCTAttcgaggaatatgcaaaaagaacagaagttccagaattttcc	Stop oligo for TPST
TPST protospacer 1	ATAGGAAGGTGGAGGACTTACAACCCATatattcctcgaaccggcggcGTTTTAGAGCTATGCTGAAAAG	TPST protospacer
TPST-comp-F	ttctctcttgtctctgttgatcacc	TPST genotyping
TPST-cutsiteF	atattcctcgaaccggcgg	TPST genotyping, anneals to protospacer 1
TPST-compR	gcgcaacagtctacgtgc	TPST genotyping
tpst-H124A oligo F	ggttagggcttgagggtgcagacagCCTAGTTGTaagcttCTTTCATCTGCTgatgacatgagcattttgagcaagatac	TPST H124A oligo
tpst-H124A oligo R	gtatcttgctcaaaatgctcatgtcatcAGCAGATGAAAGaagcttACAACTAGGctgtctgcaccctcaagccctaacc	TPST H124A oligo
tpst-R81A oligo F	ggaaaattctggaacttctgttctttttgcatattcctGCTACTGGAGGACGAacttatcaccagtggtatggatttact	TPST R81A oligo
tpst-R81A oligo R	agtaaatccataccactggtgataagtTCGTCCTCCAGTAGCaggaatatgcaaaaagaacagaagttccagaattttcc	TPST R81A oligo
tpst-R144A oligo F	gcatctgttgtaacgaatttgGCTAATCCTGTTAACCGAgtgttgagcacctatgagttttcagtggaagttgctgctcg	TPST R144A oligo

tpst-R144A oligo R	cgagcagcaacttccactgaaaactcataggtgctcaacacTCGGTTAACAGGATTAGCcaaattcgttacaacagatgc	TPST R144A oligo
tpst-S152A oligo F	agcatctgttgtaacgaatttgcgcaacCCTGTTAACcgtgtgttgGCTacctatgagttttcagtggaagttgctgctc	TPST S152A oligo
tpst-S152A oligo R	gagcagcaacttccactgaaaactcataggtAGCcaacacacgGTTAACAGGgttgcgcaaattcgttacaacagatgct	TPST S152A oligo
TPST protospacer 2	ATAGGAAGGTGGAGGACTTACAACCCATtgctcaacacacgattcactgttttagagctatgctgaaaag	Protospacer for *tpst-R144A*
TPST protospacer 3	ATAGGAAGGTGGAGGACTTACAACCCATgaagacaaaagcttgcagctgttttagagctatgctgaaaag	Protospacer for *tpst-H124A*
TPST-gt-F1	caaagtatcagcagcaccacc	Genotyping for *tpst-R81A*
TPST-gt-R1	gtgagatccttcgcttcccaata	Genotyping for *tpst-R81A*
TPST-gt-F2	cgtgcaggtacagctctagg	Genotyping for *tpst-H124A* and *tpst-R144A*
TPST-gt-R4	gtaagcaaaggagaacatgccc	Genotyping for *tpst-H124A* and *tpst-R144A*
TPST-gt-R2	tgaagacaaaagcttgcagctg	Genotyping, anneals to protospacer 2
TPST-gt-R3	tgctcaacacacgattcactgg	Genotyping, anneals to protospacer 3
TPST-R81A-R	ccactggtgataagtTCGTCC	Genotyping, anneals to *tpst-R81A*
TPST-H124A-R	caaaatgctcatgtcatcAGCAGATG	Genotyping, anneals to *tpst-H124A*
TPST-R144A-F	gttgtaacgaatttgGCTAATCCTGT	Genotyping, anneals to *tpst-R144A*